PROCEEDINGS OF SCIENCE

Fourier Acceleration of SU(3) Pure Gauge Theory at Weak Coupling

Yi-Kai Huo[a,*] **and Norman Christ**[a]

[a] *Physics Department, Columbia University, New York, NY 10027, USA*

E-mail: yh3285@columbia.edu, nhc@phys.columbia.edu

In the hybrid Monte Carlo simulation of SU(3) pure gauge theory, we explore a Fourier acceleration algorithm to reduce critical slowing down. By introducing a soft-gauge-fixing term in the action, we can identify the eigenmodes in the weak-coupling expansion of the action and eliminate the differences in their evolution frequencies. A special unit-link boundary, in which the links lying in the boundary faces are fixed to be unit matrices, is also proposed to eliminate the $\mathbf{Z}_3$ symmetry and the tunneling between $\mathbf{Z}_3$ phases in which is not of interest here. We present the theoretical details and the numerical implementation of this algorithm, compare the autocorrelation times of certain observables with the usual hybrid Monte Carlo algorithm to show its acceleration effect for weak coupling and examine its potential application to physically relevant lattice spacings.

The 40th International Symposium on Lattice Field Theory (Lattice 2023)
July 31st - August 4th, 2023
Fermi National Accelerator Laboratory

*Speaker

PoS(LATTICE2023)042

1. Introduction

As the lattice spacing becomes closer to zero, more Molecular Dynamics (MD) time units are required to generate an independent configuration using the hybrid Monte Carlo (HMC) algorithm in lattice QCD. This is driven by the disparity in the evolution velocities of different modes. A smaller lattice spacing leads to a higher upper limit of high-frequency modes, which requires a smaller time step to carry out precise integration. However, such a smaller time step will consequently increase the number of time steps required to evolve the long-distance modes. This slowing-down effect of gauge configuration evolution is commonly known as critical slowing down (CSD).

Since at weak coupling the gauge field enter the dominant term in the action quadratically, the interaction among fields will be similar to the harmonic oscillators in a weak coupling expansion. This inspires us to develop a Fourier acceleration method to reduce the effects of critical slowing down. Different from the conventional HMC algorithm, we construct a new kinetic energy term including mass terms which are proportional to the coupling strengths of the various modes. This adjustment can result in all modes having the same frequency. However, direct identification of the modes of the Wilson action poses challenges due to the local gauge symmetry of the Yang-Mills theory. To address this issue, we introduce a gauge-fixing term which allows the identification of different modes in Fourier space in a weak coupling expansion. One prior paper has discussed the theoretical approaches to utilize this Gauge-Fixed Fourier Acceleration (GFFA) algorithm [1], while another one presented the numerical results with periodic boundary conditions and frozen-link boundary conditions [2]. This article introduces new unitary-link boundary conditions and covers both the theoretical implementation and numerical outcomes of GFFA within this framework.

2. Gauge-Fixing Action

To identify different Fourier modes, we introduce the following soft gauge-fixing term. Unlike the strict enforcement of the Landau condition, our approach involves constraining the field's evolution within an region around Landau gauge. Samples which are far from this region will be highly improbable since they will be suppressed by an exponential factor,

$$S_{\mathrm{GF}}[U] = -\frac{1}{3}\beta M^2 \sum_{n,\mu} \mathrm{ReTr}[U_\mu(n)], \tag{1}$$

where M is a mass-like parameter to determine the strength of restriction around Landau gauge. This soft gauge-fixing term was initially introduced to approximate Landau gauge without Gribov copies [3, 4].

To leave gauge-invariant observables unchanged, we need to introduce a corresponding Fadev-Poppov term [1],

$$S_{\mathrm{FP}}[U] = \ln \int \mathrm{d}g \exp\left(\frac{1}{3}\beta M^2 \sum_{n,\mu} \mathrm{ReTr}[U^g_\mu(n)]\right). \tag{2}$$

Hence, we obtain our total action,

$$S = S_{\mathrm{W}} + S_{\mathrm{GF}} + S_{\mathrm{FP}}, \tag{3}$$

where S_{W} is the usual Wilson action.

According to the study of this action in the continuum, we can decompose the field into transverse and longitude modes in Fourier space [5]. Consequently, we construct the corresponding kinetic term in our HMC molecular dynamics Hamiltonian, to accelerate low-energy modes:

$$\begin{aligned} H_{\text{kinetic}} &= \sum_k \text{Tr}\left[P_\mu(-k)D^{\mu\nu}(k)P_\nu(k)\right], \\ D_{\mu\nu}(k) &= \frac{1}{k^2}P^{\text{T}}_{\mu\nu}(k) + \frac{1}{M^2}P^{\text{L}}_{\mu\nu}(k), \\ \text{P}^{\text{T}}_{\mu\nu}(k) &= \delta_{\mu\nu} - \frac{k_\mu k_\nu}{k^2}, \text{P}^{\text{L}}_{\mu\nu}(k) = \frac{k_\mu k_\nu}{k^2}, \end{aligned} \tag{4}$$

where $\text{P}^{\text{T}}_{\mu\nu}(k)$ and $\text{P}^{\text{L}}_{\mu\nu}(k)$ are projection operators onto the transverse and longitude modes, respectively. In the kinetic term, we introduce the "mass" terms which are the inverse of the quadratic parts of the weak coupling expansion of our gauge-fixed action.

Analogously, for a general 4-dimensional finite-volume lattice, where the allowed positions $n = (n_0, n_1, n_2, n_3)$ obey $0 \le n_\mu \le N_\mu, 0 \le \mu \le 3$, we can write down the finite-volume form of our gauge-fixed action of $4N_0N_1N_2N_3$ gauge variables $A_\mu(n)$, in the weak coupling limit, as

$$S_{\text{FV}}[U] = \frac{\beta}{12}\sum_n \left(M^2 \left(\nabla^{\text{t}}_\mu A_\mu\right) \frac{1}{\nabla^{\text{t}}\nabla} \left(\nabla^{\text{t}}_\nu A_\nu\right) + \frac{1}{2}\sum_{\mu,\nu} \left(\nabla_\mu A_\nu - \nabla_\nu A_\mu\right)^2 \right), \tag{5}$$

where the blue right-most term on the right-hand side is the leading term in the weak-coupling expansion of the Yang-Mills gauge action and the left-most red term on the right-hand side is the corresponding gauge-fixing part. The quantities ∇_μ and ∇^{t}_μ are linear operators corresponding to forward and backward discrete derivatives.

$$\left[\nabla_\mu \Lambda\right](n) = \Lambda(n+\hat{\mu}) - \Lambda(n), \qquad \left[\nabla^{\text{t}}_\mu \Lambda\right](n) = \Lambda(n-\hat{\mu}) - \Lambda(n). \tag{6}$$

3. Unit-Link Boundary Conditions and Finite-Volume Eigenmodes

Standard Fourier transformation can be used to identify the eigenmodes in the weak coupling expansion of the gauge-fixed action in the continuum theory [5]. To implement Fourier acceleration on a discrete finite-volume lattice, we should first identify the eigenmodes of the discrete action outlined in Eq. 5. Our previous work has successfully identified eigenmodes of finite-volume discrete action with periodic boundary conditions [2]. Furthermore, our earlier numerical experiments revealed unwelcome different behaviors between the HMC algorithm applied to the Wilson action and the gauge-fixed action. Specifically, the HMC with the Wilson action displayed frequent tunneling among the Polycov phases due to its $\mathbf{Z}_3$ symmetry. In the contrast, HMC with the gauge-fixed action remained confined to one of the three cubic roots of identity and tunneled very infrequently. This behavior stems from the considerable computational demand involved in accurately calculating the force of the Faddeev-Popov term, which necessitates a large number of heatbath inner Monte Carlo samples [2]. To eliminate potential effects arising from this $\mathbf{Z}_3$ phase tunneling on our autocorrelation analysis, we propose the following solution: freezing the links along the edges of the lattice. Unit-link boundary conditions serve as a comprehensive strategy to tackle these challenges. This approach prevents the links from tunneling to other phases, effectively addressing both the need to determine the weak-coupling eigenmodes and the $\mathbf{Z}_3$ symmetry issue simultaneously.

Unit-link boundary conditions require that the gauge field should vanish at the lattice's edge:

$$\begin{cases} U_\mu(n)|_{n_\rho=0} = U_\mu(n)|_{n_\rho=N_\rho} = 1 \\ A_\mu(n)|_{n_\rho=0} = A_\mu(n)|_{n_\rho=N_\rho} = 0 \end{cases} \quad \text{for} \quad \rho \neq \mu. \tag{7}$$

With unit-link boundary conditions, the modes are no longer plane waves. To comply with the boundary conditions, we should tailor the modes $A_\mu(k,n)$ as combinations of those plane waves. Given that the gauge field vanishes at the lattice's edge, we easily deduce that position-dependence of the μ-component of a mode in the three directions different from μ,

$$A_\mu(k,n) \propto \prod_{\substack{\rho=0 \\ \rho\neq\mu}}^{3} \sqrt{\frac{2}{N_\rho}} \sin(k_\rho n_\rho), \tag{8}$$

where $k = \frac{\pi}{N}\ell$, the integer ℓ_ρ obeys $1 \leq \ell_\rho \leq N_\rho - 1$. To determine the residual spatial dependence of the direction μ, we consider a gauge transformation on the zero field which is generated by

$$\Lambda(n,k) = \prod_{\rho=0}^{3} \sin(k_\rho n_\rho). \tag{9}$$

The gauge field after this transformation will still obey our unit-link boundary conditions. Hence, we can obtain a zero mode of the Yang-Mills action obeying our unit-link boundary conditions. We call it the longitudinal mode $A_{\mathrm{L},\mu}(k,n)$:

$$A_{\mathrm{L},\mu}(k,n) = \varepsilon_{\mathrm{L},\mu}(k) \cos\left(k_\mu\left(n_\mu + \frac{1}{2}\right)\right) \prod_{\substack{\rho=0 \\ \rho\neq\mu}}^{3} \sin(k_\rho n_\rho), \qquad \varepsilon_{\mathrm{L},\mu}(k) \quad = \sin\left(\frac{k_\mu}{2}\right), \tag{10}$$

where $\varepsilon_{\mathrm{L},\mu}$ is the polarization vector, $k = \frac{\pi}{N}\ell$, the integer ℓ_μ obeys $0 \leq \ell_\mu \leq N_\mu - 1$ and the integer ℓ_ρ obeys $1 \leq \ell_\rho \leq N_\rho - 1$. The remaining three transverse modes $A_{T_i,\mu}(k,n)$, for $1 \leq i \leq 3$ can be constructed from three transverse polarization vectors $\varepsilon_{T_i,\mu}(k)$ which are orthogonal to $\varepsilon_{L,\mu}(k)$ and to each other:

$$\sum_{\rho=0}^{3} \varepsilon_{T_i,\rho}(k)\varepsilon_{T_j,\rho}(k) = \delta_{ij}, \qquad \sum_{\rho=0}^{3} \quad \varepsilon_{T_i,\rho}(k)\varepsilon_{L,\rho}(k) = 0 \text{ for } 1 \leq i \leq 3. \tag{11}$$

Actually, we needn't make a specific choice of these $\varepsilon_{T_i,\mu}(k)$ polarization vectors. All of these transverse modes have the same eigenvalue of Yang-Mills action:

$$\lambda_T = 4 \sum_{\mu=0}^{3} \sin^2\left(\frac{k_\mu}{2}\right). \tag{12}$$

Finally, we obtain a complete set of eigenmodes of Wilson action:

$$A_{X,\mu}(k) = \varepsilon_{X,\mu} \sqrt{\frac{2}{N_\mu}} \cos\left(k_\mu\left(n_\mu + \frac{1}{2}\right)\right) \prod_{\substack{\rho=0 \\ \rho\neq\mu}}^{3} \sqrt{\frac{2}{N_\rho}} \sin(k_\rho n_\rho), \tag{13}$$

where $X = L, T_1, T_2, T_3$ labels the different modes, $\varepsilon_{X,\mu}$ is polarization vector, $k = \frac{\pi}{N}\ell$, the integer ℓ_μ obeys $0 \le \ell_\mu \le N_\mu - 1$ and the integer ℓ_ρ obeys $1 \le \ell_\rho \le N_\rho - 1$.

Instead of Fourier transformation, we apply the following discrete sine and cosine transformation between the field $A_\mu(n)$ in position space and the field $\widetilde{A}_\mu(k)$ in wave number space:

$$\begin{aligned}\widetilde{A}_\mu(k) &= \sum_{n_\mu=0}^{N_\mu-1} \sum_{\substack{n_\rho=1 \\ \rho\neq\mu}}^{N_\rho-1} A_\mu(n)\psi(n,\ell)_\mu, \\ \psi(n,\ell)_\mu &= \sqrt{\frac{2}{N_\mu}} \cos\left(\frac{\pi}{N_\mu}\ell_\mu\left(n_\mu+\frac{1}{2}\right)\right) \prod_{\substack{\rho=0 \\ \rho\neq\mu}}^{3} \sqrt{\frac{2}{N_\rho}} \sin(\frac{\pi}{N_\rho}\ell_\rho n_\rho).\end{aligned} \tag{14}$$

4. Fourier Acceleration

Based on the above finite-volume eigenmodes, we can rewrite the finite volume expansion of our gauge-fixed action:

$$S_{\mathrm{FV}}[U] \approx \frac{\beta}{12} \sum_{k,\mu,\nu} \widetilde{A}_\mu(k) \left(4\left(\sum_{\mu=0}^{3} \sin^2\left(\frac{k_\mu}{2}\right)\right) \mathrm{P}^{\mathrm{T}}_{\mu\nu,\mathrm{FV}} + M^2 \mathrm{P}^{\mathrm{L}}_{\mu\nu,\mathrm{FV}}\right) \widetilde{A}_\nu(k), \tag{15}$$

where $\mathrm{P}^{\mathrm{T}}_{\mu\nu,\mathrm{FV}}$ and $\mathrm{P}^{\mathrm{L}}_{\mu\nu,\mathrm{FV}}$ are the corresponding projection operators for the transverse modes and longitudinal modes:

$$\mathrm{P}^{\mathrm{T}}_{\mu\nu,\mathrm{FV}} = \delta_{\mu\nu} - \frac{\sin\left(\frac{k_\mu}{2}\right)\sin\left(\frac{k_\nu}{2}\right)}{\sum_{\mu=0}^{3}\sin^2(\frac{k_\mu}{2})}, \qquad \mathrm{P}^{\mathrm{L}}_{\mu\nu,\mathrm{FV}} = \frac{\sin\left(\frac{k_\mu}{2}\right)\sin\left(\frac{k_\nu}{2}\right)}{\sum_{\mu=0}^{3}\sin^2(\frac{k_\mu}{2})}. \tag{16}$$

Finally, we can construct the following kinetic term to implement Fourier acceleration where the coefficients of the conjugate momenta are chosen to be the inverses of the coefficients of gauge fields in the weak coupling limit of the gauge action:

$$\begin{aligned}H_{\mathrm{kinetic,FV}} &= \sum_k \mathrm{Tr}\left(\widetilde{p}_\mu(k)\ \mathrm{D}^{\mu\nu}_{\mathrm{FV}} \widetilde{p}_\nu(k)\right) \\ \mathrm{D}^{\mu\nu}_{\mathrm{FV}} &= \frac{1}{4\left(\sum_{\mu=0}^{3}\sin^2\left(\frac{k_\mu}{2}\right)\right)} \mathrm{P}^{\mathrm{T}}_{\mu\nu,\mathrm{FV}} + \frac{1}{M^2}\mathrm{P}^{\mathrm{L}}_{\mu\nu,\mathrm{FV}}.\end{aligned} \tag{17}$$

With this choice of kinetic term, the weak coupling expansion of the Hamiltonian will be analogous to a set of harmonic oscillators in wave number space with the same frequency for all of the modes:

$$\begin{aligned}H = S + H_{\mathrm{kinetic}} \approx \frac{1}{2}\sum_{k,\mu} \frac{\left(\widetilde{p}^L_\mu(k)\right)^2}{M^2} + \frac{1}{2}\sum_{k,\mu} M^2 \left(\widetilde{A}^L_\mu(k)\right)^2 \\ + \frac{1}{2}\sum_{k,\mu} \frac{\left(\widetilde{p}^T_\mu(k)\right)^2}{4\left(\sum_{\mu=0}^{3}\sin^2\left(\frac{k_\mu}{2}\right)\right)} + \frac{1}{2}\sum_{k,\mu} 4\left(\sum_{\mu=0}^{3}\sin^2\left(\frac{k_\mu}{2}\right)\right)\left(\widetilde{A}^T_\mu(k)\right)^2.\end{aligned} \tag{18}$$

5. Numerical Experiments

In order to show the acceleration effect on the generation of independent gauge configurations, we do both original HMC and GFFA simulations on two different lattice volumes, 8^4 and 16^4, at $\beta = 10$, and compare integrated auto-correlation times τ_{int} of plaquette values U_{P}:

$$\tau_{int} = \frac{1}{2} + \sum_{\Delta=1}^{\Delta_{cut}} C(\Delta), \qquad C(\Delta) = \left\langle \frac{(U_{\mathrm{P}}(t) - \bar{U}_{\mathrm{P}})(U_{\mathrm{P}}(t+\Delta) - \bar{U}_{\mathrm{P}})}{\sigma^2} \right\rangle_t , \tag{19}$$

where $\bar{U}_P$ is the value of the average plaquette and σ is its standard deviation.

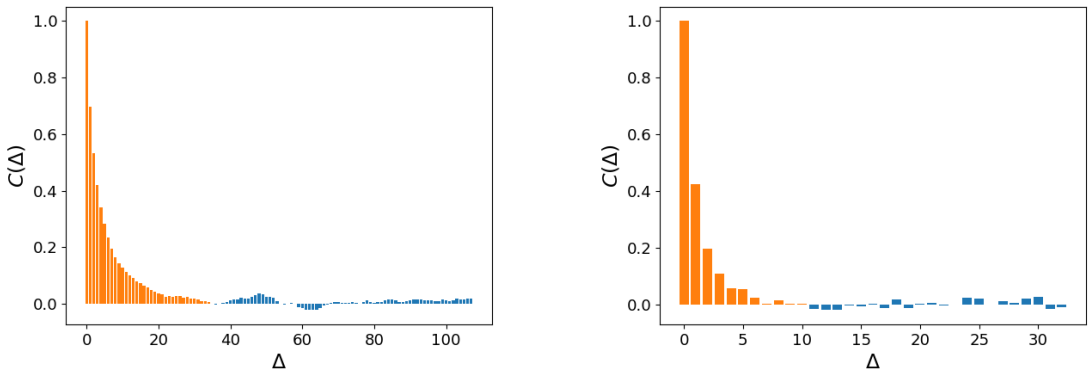

(a) HMC run with traj length set to 0.6 and 19900 trajs

(b) GFFA run with traj length set to 0.6 and 2184 trajs

Figure 1: Auto-correlation function of the plaquettes on a 16^4 lattice with unit-link boundary conditions, which reveals reduced autocorrelation in the case of GFFA

Our results, shown in Tables 1 and 2, indicate that a factor of 4× acceleration is achieved by GFFA as opposed to HMC. In these tables, 'traj L' refers to trajectory length in MD time units, 'MDsteps' represents the number of molecular dynamics leap-frog steps in each trajectory, and auto-correlation times are reported in molecular dynamics time units.

β	size	traj num	traj L	MDsteps	plaquette	plaq τ_{int}
10	8^4	19940	0.6	24	0.85094(81)	5.38(35)
10	16^4	19900	0.6	64	0.81900(22)	4.64(33)

Table 1: HMC results for the Wilson action with unit-link boundary conditions.

β	size	M	traj num	traj L	MDsteps	plaquette	plaq τ_{int}
10	8^4	3.0	3924	0.6	48	0.85090(84)	1.22(10)
10	16^4	3.0	2184	0.6	64	0.81903(23)	1.36(18)

Table 2: Results for the Fourier-accelerated HMC with the gauge-fixed action with unit-link boundary conditions. Integrated auto-correlation times are reported in molecular dynamics time units. They are defined to be the area under the curves shown in Figure. 1 up to the value of Δ when the auto-correlation function changes sign.

While the usual HMC accept-reject step is possible in the GFFA algorithm, the change in the energy after a single trajectory requires a stochastic evaluation of ΔS_{FP} which is very difficult to sample. Therefore, as implemented our GFFA algorithm is not exact and requires choosing a time step that is sufficiently small that the finite time step integration errors can be ignored. The plaquette column in Tables 1 and 2 is presented to show the accuracy of the GFFA algorithm whose autocorrelation times are being shown.

6. Conclusion and Outlook

This article extends our prior investigations into the Fourier acceleration of SU(3) pure gauge theory. We have introduced unit-link boundary conditions to address subtleties encountered in previous numerical experiments. We have derived the finite-volume action within the weak coupling limit and identified the corresponding exact Fourier modes. Our numerical experiments, conducted with two different lattice volumes, demonstrate an acceleration factor of $\times 4$ for plaquettes achieved by GFFA compared to the original HMC method.

Moving forward, our future work encompasses several key aspects. Firstly, we plan to calculate Wilson flow variables to further test the algorithm's acceleration efficiency on long-distance quantities. Secondly, we aim to generate configurations with smaller β to explore the practical limit of the algorithm's effectiveness. Additionally, we intend to experiment with implementing the algorithm on large-volume lattices by subdividing them into smaller volumes and applying Fourier acceleration independently to sub-volumes in a checkerboard fashion. Finally, in pursuit of a long-term goal, we aim to include fermion determinants and investigate the algorithm's efficiency in reducing critical slowing down when dealing with dynamical fermions.

Acknowledgements

We would like to thank our RBC/UKQCD collaborators for numerous discussions and helpful suggestions and particularly Peter Boyle, Chulwoo Jung and Chris Kelly for help with Grid and other software issues. This research was supported by the Exascale Computing Project (17-SC-20-SC), a collaborative effort of the U.S. Department of Energy Office of Science and the National Nuclear Security Administration.

References

[1] Y. Zhao, *Numerical Implementation of Gauge-Fixed Fourier Acceleration*, PoS **LATTICE2018**, (2019)026, [hep-lat/1812.05790].

[2] A. Sheta, Y. Zhao and N. H. Christ, *Gauge-Fixed Fourier Acceleration*, PoS **LATTICE2021**, (2022)084, [hep-lat/2108.05486].

[3] D. Zwanziger, *Quantization of Gauge Fields, Classical Gauge Invariance and Gluon Confinement*, Nucl. Phys. B **345** (1990), 461-471

[4] S. Fachin and C. Parrinello, *Global gauge fixing in lattice gauge theories*, Phys. Rev. D **44** (1991), 2558-2564

[5] S. P. Fachin, *Quantization of Yang-Mills theory without Gribov copies: Perturbative renormalization*, Phys. Rev. D **47** (1993), 3487-3495